

High Voltage CMOS Bidirectional Current Sensor for Battery Monitoring in Portable Devices

Chua-Chin Wang
 Dept. Elec. Eng./Inst. Undersea Tech.
 National Sun Yat-Sen Univ.
 Kaohsiung, Taiwan
 ccwang@ee.nsysu.edu.tw

Pang-Yen Lou
 Dept. of Electrical Eng.
 National Sun Yat-Sen Univ.
 Kaohsiung, Taiwan
 lou105cat@vlsi.ee.nsysu.edu.tw

Zong-You Hou
 Dept. of Electrical Eng.
 National Sun Yat-Sen Univ.
 Kaohsiung, Taiwan
 blazesky@vlsi.ee.nsysu.edu.tw

Hsiu-Chun Tsai
 Dept. of Electrical Eng.
 National Sun Yat-Sen Univ.
 Kaohsiung, Taiwan
 roytsai94@vlsi.ee.nsysu.edu.tw

Yi-Jen Chiu
 Dept. of Photonics
 National Sun Yat-Sen Univ.
 Kaohsiung, Taiwan
 yjchiu@faculty.nsysu.edu.tw

Yu-Cheng Lin
 Dept. of Engineering Science
 National Cheng Kung Univ.
 Tainan, Taiwan
 yuclin@mail.ncku.edu.tw

Abstract—This investigation demonstrates a high-accuracy bidirectional high-voltage (HV) current sensor fabricated by CMOS technology. Besides Noise filter, Sense stage, and Controller, the proposed current sensor is featured with a Switching Network composed of transmission gates, which is able to steer the direction of the current. A digital feedback loop comprises Controller generating a pair of digital signals to Switching Network such that the direction of the current is detected real time. The area of the proposed sensor on silicon is $1173 \times 664 \text{ } \mu\text{m}^2$ using $0.5 \text{ } \mu\text{m}$ high-voltage CMOS process, which is very compact to be easily integrated in any portable devices demanding a current monitoring function. The sensing voltage error is 0.7% by the physical measurements, where the input voltage range is $8 \sim 14 \text{ V}$, and the current sensing range is $-3 \sim 3 \text{ A}$.

Keywords—high-voltage (HV), bidirectional, input voltage range, current sensor, sensing error

I. INTRODUCTION

In any power system, particularly those devices with portability demand due to the usage of batteries, bidirectional current detection is very important for safety [1]. Traditional current sensors are found very hard to detect the bidirectional current at the same time such that detecting the bidirectional current with high accuracy attracts strong attention [2]-[5]. Many researchers have reported several current sensor designs to resolve this issue, e.g., [6]-[8], basically using a low-resistance resistor as a sensing resistor in series with the load and then detecting the voltage drop thereof. Although the low-resistance resistors means to improve efficiency and accuracy, the intrinsic resistance variation results in large input offset to amplifiers [9]. Besides, to the best of our survey, all of the existing current sensors are focused on the detection of one current direction. That is, they are not able to detect the discharge and charge currents of a battery system at the same time, unless two sensors are used simultaneously. To resolve all the mentioned problems, a bidirectional current sensor using the fully-differential amplifier (FDA) with digital auxiliary circuits is proposed in this investigation. More specifically, the proposed sensor is featured with a digital feedback loop, where the sensed output voltage is sampled and converted into digital codes to drive Switching Network composed of transmission gates such that the correct current direction can be detected and steered. The Switching Network not only correct the direction of the current, but also make the circuit more accurate than many prior works. The design was realized on silicon prototype and justified by physical measurements to sense the voltage from $8 \sim 14 \text{ V}$, and current

range from -3 A to 3 A . The most important of all is that only 0.7% error is measured on silicon to prove the accuracy of the proposed design.

II. HIGH-VOLTAGE BIDIRECTIONAL CURRENT SENSOR

A. System Architecture and Operation

The block diagram of the proposed HV bidirectional current sensor is shown in Fig. 1, including a current sensing resistor R_{cs} , a Noise filter, a Switching Network, a Sense Stage, R_{out} , and a Controller.

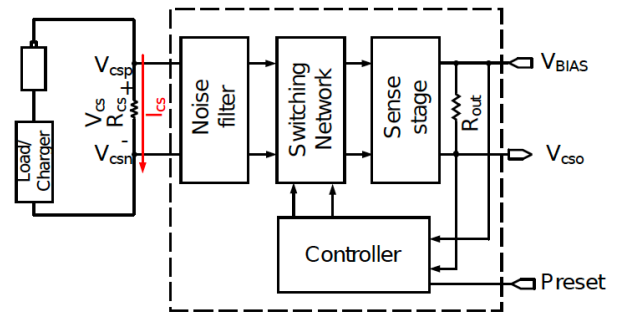


Fig. 1: System diagram of the proposed design

Fig. 2 shows the schematic of the proposed HV bidirectional current sensor. A very small sensing voltage (V_{cs}) is generated by I_{cs} via R_{cs} namely, a small resistor, as shown in Fig. 1. Noise filter comprising $4 R_{NF}$ s, and a C_{NF} rejects unwanted high-frequency noise. Noise filter acts like a low-pass filter with a 3-dB bandwidth defined in Eqn. (1).

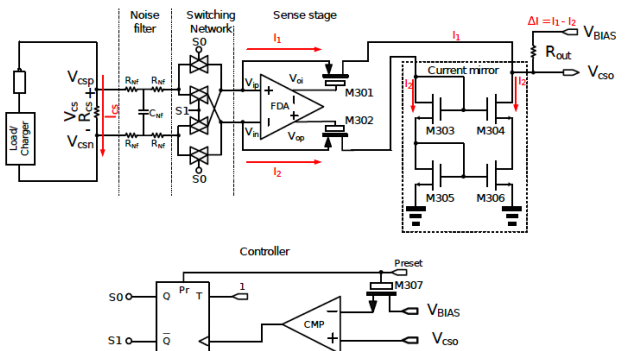


Fig. 2: Schematic of the proposed HV current sensor

$$f_{-3dB} = \frac{1}{2\pi \cdot R_{Nf} \cdot C_{Nf}} \quad (1)$$

FDA in Sense Stage of Fig. 2 is designed to attain a virtual short across the input terminals (namely, $V_{ip} \sim V_{in}$). The drain currents of the M301 and M302 are then proportional to $(V_{csp}-V_{in})/2xR_{Nf}$ and $(V_{csn}-V_{ip})/2xR_{Nf}$, respectively, assuming the transmission gates are ideal. Current mirror carries out the current subtraction to generate $\Delta I = I_1 - I_2$, whereupon ΔI is converted into an output voltage, V_{cso} , by Rout. Battery system's operations are classified into two modes:

- Discharge mode: When $V_{csp} > V_{csn}$ makes $I_1 > I_2$, the controller turns on S0, and then V_{BIAS} is kept higher than V_{cso} to inject current into the current mirror.
- Charge mode: When $V_{csp} < V_{csn}$ makes $I_1 < I_2$, the controller turns on S1, and then V_{BIAS} is lower than V_{cso} . The current would be steered from V_{cso} to V_{BIAS} .

B. Derivation of Current Sensing

Assume the gain of the entire system is A_v . V_{cso} can be formulated as Eqn. (2), where A_v can be written as Eqn. (3). Thus, V_{cso} can be easily organized as Eqn. (4). Therefore, I_{cs} can be estimated indirectly using V_{cso} as shown in Eqn. (5).

$$V_{cso} = V_{cs} \cdot A_v + V_{BIAS} \quad (2)$$

$$A_v = \frac{R_{out}}{2 \cdot R_{Nf}} \quad (3)$$

$$V_{cso} = \frac{V_{cs} \cdot R_{out}}{2 \cdot R_{Nf}} + V_{BIAS} \quad (4)$$

$$I_{cs} = \frac{V_{cs}}{R_{cs}} = \frac{(V_{cso} - V_{BIAS}) \cdot 2 \cdot R_{Nf}}{R_{out} \cdot R_{cs}} \quad (5)$$

C. FDA Design

FDA is basically a two-stage fully-differential amplifier including a common-mode feedback, as shown in Fig. 3. Apparently, the common-mode voltage affects the output swing. Since the proposed sensor is meant to detect high voltage and current, which will easily generate significant common-mode offset. Thus, common-mode feedback circuit is needed, which regulates its common-mode voltage to a pre-defined value.

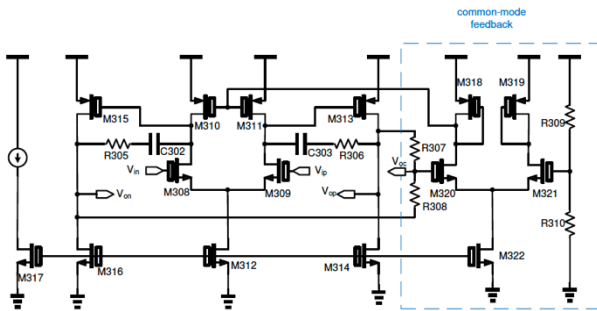


Fig. 3: FDA design [10]

D. Controller Design

Referring to Fig. 2 again, Controller comprises a comparator (CMP) and a T flip-flop. The operation is listed as follows.

- (1). T flip-flop is driven by Preset being high to pull up S0 high. Then, the Preset would be low.
- (2). CMP compares V_{cso} with V_{BIAS} to determine which switch to turn on. When V_{BIAS} is higher than V_{cso} , S0 is kept unchanged. On the contrary, T flip-flop pull high S1, and S0 is pulled low.
- (3). When S0 turns off, and S1 turns on, Preset would change to be high.
- (4). The output of CMP is used as the clock of T flip-flop. When the current direction changes, the output of the T flip-flop is reversed to flip the states of those transmission gates in Switching Network.

III. IMPLEMENTATION AND MEASUREMENT

Most of the portable devices are powered with rechargeable batteries, which are mainly suffered from the noise interference in low frequency. Thus, to reject the high-frequency noise higher than 1.5 MHz, $R_{Nf} = 10$ k ohm, and $C_{Nf} = 20$ pF are used in the Noise filter as shown in Eqn. (1). To enlarge the range of the sensor current, the smallest R_{cs} in the process is selected to be 0.067 ohm in our design. Referring to Eqn. (2), a linear function is expected between V_{cso} and V_{cs} . Fig. 4 shows the simulation between V_{cs} and V_{cso} to verify this feature, when the sensed voltage V_{cs} range is $-200 \sim 200$ mV, and V_{BIAS} is 5 V.

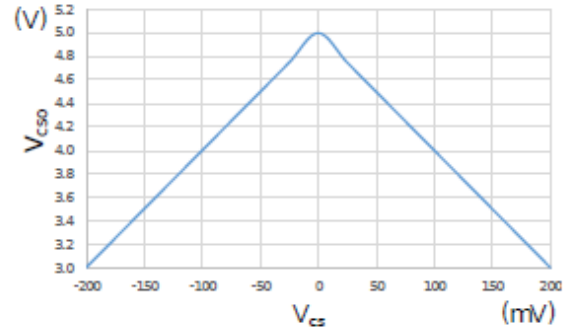


Fig. 4: V_{cs} vs. V_{cso}

A. System Validation and Chip Implementation

The proposed current sensor was fabricated using TSMC 0.5 um CMOS high-voltage mixed-signal based LDMOS USG AL 2P3M polycide (T50UHV). Fig. 5 shows the die photo of the proposed HV current sensor, where the chip area is $1744 \times 1303 \mu m^2$, and the core area is $1173 \times 664 \mu m^2$.

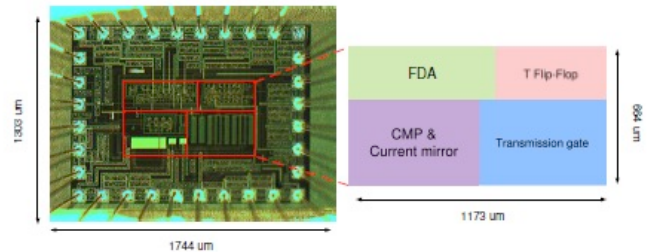


Fig. 5: Die photo of the proposed HV current sensor

Fig. 6 is the all-PVT-corner (process, voltage, temperature) post-layout simulation of the proposed current sensor to validate Eqn. (5). It shows that when the sensing current range is $-3 \sim 3$ A, the output voltage range V_{CSO} is $3 \sim 5$ V. The proposed HV current sensor shows the worst-case sensing error of 0.85 % when I_{CS} equals to ± 3 A, as shown in Fig. 7. Besides, the average error is 0.48 %.

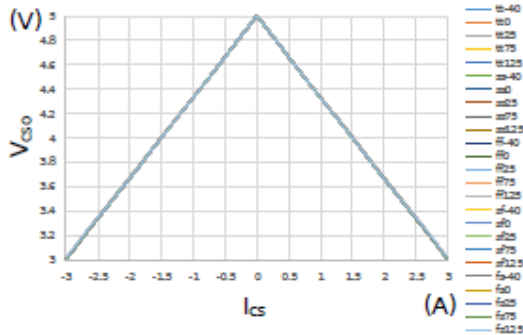


Fig. 6 : All-PVT-corner post-layout simulation

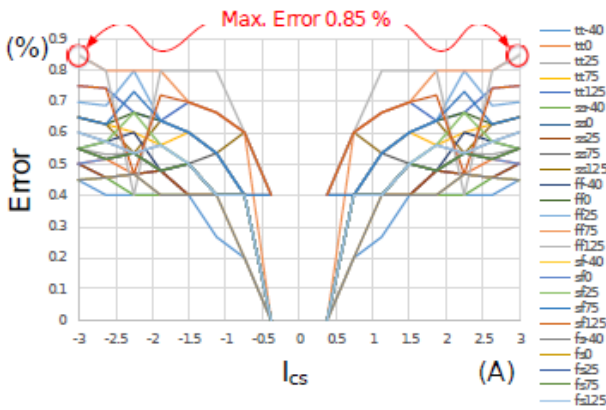


Fig. 7: Sensing current error distribution

B. Measurement and Performance Analysis

To prove the performance of the proposed sensor working in the range of $8 \sim 14$ V, the power supply generates 7 voltages (8, 9, 10, 11, 12, 13, 14 V). The ANR26650 battery module is the real battery device to be tested [11], where the current magnitude is adjusted via an electronic load (PRODIGT 3311D Electronic Load). Meanwhile, the electronic load consumes 13 different currents in the range of $0 \sim 3$ A, as shown in Fig.8. Fig. 9 summarizes the error distribution at the 7 sensed voltages given the same current. The worst measured error is less than 1.22 %.

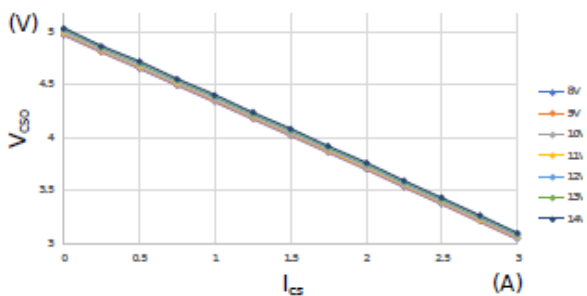


Fig. 8: Measurement results by the proposed sensor

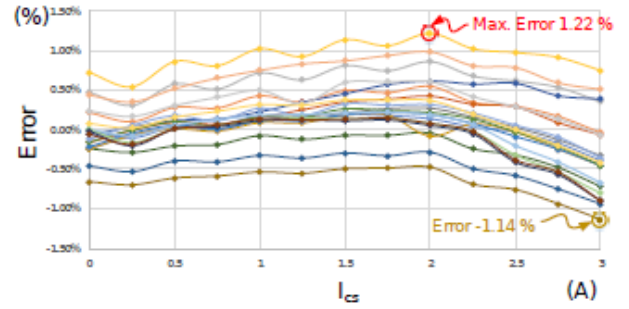


Fig. 9: V_{CSO} error distribution

C. Reliability and Repeatability Measurement

Besides the experiment using equipment as the above, we use a real battery module consisting of 4S3R ANRANR26650 cells for the field test. A battery testing system (LANHE CT2001D) was used to charge/discharge the battery module to verify the bidirectional current sensing. Three chips were used to carry out a total of 225 times measurements as summarized in Fig. 10. The standard deviation in the measurement results is smaller than $\pm 3\sigma$, as shown in Fig. 10.

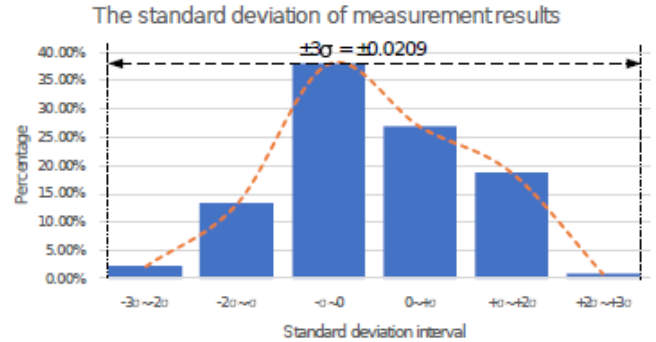


Fig. 10: Standard deviation of 225 times measurements

A typical FOM is defined as follows to give a fair measure for all kinds of current sensing approaches. Our design attains the best FOM of all the works as shown in Table I.

$$FOM = \frac{\text{Voltage Range} \times \text{Sensing Current Range}}{\text{Core area} \times \text{Max. Error}}$$

IV. CONCLUSION

This investigation presents a high-accuracy CMOS HV bidirectional current sensor. Our design works in the input voltage range from $8 \sim 14$ V. Moreover, it attains the very small sensing voltage error $< 0.7\%$. The design is featured with the digital feedback control to make high accuracy and bidirectional sensing feasible at the same time.

ACKNOWLEDGMENT

This research was partially supported by Ministry of Science and Technology under grant MOST 108-2218-E-110-011- and MOST~107-2218-E-110-002-. The authors would like to express their gratefulness to TSRI (Taiwan Semiconductor Research Institute) of NARL (Nation Applied Research Laboratories), Taiwan, for the chip fabrication service.

REFERENCES

- [1] T. Dong, J. Li, and H. Dai, "Analysis on the influence of measurement precision of the battery management system on the state of charge estimation," in Proc. Asia-Pacific Power and Energy Engineering Conference (APPEEC), pp. 1-5, Mar. 2010.
- [2] H. Q. Tay, V. T. Nam, N. H. Duc and B. N. Chau, "A current sensing circuit using current-voltage conversion for PMOS-based LDO regulators," in Proc. 2012 International Symposium on Computer Applications and Industrial Electronics (ISCAIE), pp. 1-4, Mar. 2012.
- [3] F. Briffod, D. Alasia, L. Thevenaz, G. Cuenoud and P. Robert, "Extreme current measurements using a fibre optics current sensor," in Proc. 2002 15th Optical Fiber Sensors Conference Technical Digest., (OFS 2002), pp. 607-610, Aug. 2002.
- [4] H. Zhou, C. Tan and J. Fletcher, "Lossless bi-directional current sense circuit for low-voltage high-current DC/DC converters," in Proc. IECON 2018 - 44th Annual Conference of the IEEE Industrial Electronics Society, pp. 1305-1308, Dec. 2018.
- [5] Y. Wu, Y. Su, G. Han, Y. Wu, Q. Yi, G. Sun and D. Wang "Research on a novel bidirectional direct current circuit breaker," in Proc. 2017 4th International Conference on Electric Power Equipment - Switching Technology (ICEPE-ST), pp. 370-374, Dec. 2017.
- [6] H. Wang, X. Hu, Q. Liu, G. Zhao, and D. Luo, "An on-chip high-speed current sensor applied in the current-mode DC-DC converter," in Proc. IEEE Transactions on Power Electronics (TPE), vol. 29, no. 9, pp. 4479-4484, Sep. 2014.
- [7] W.-J. Lu, S.-S. Wang, M.-Y. Tseng, and C.-C. Wang, "A capacity monitoring system with HV current sensor and calibrated current estimation approach," in Proc. IEEE Region 10 Conference (TENCON), pp. 1-4, Nov. 2015.
- [8] K. Itoh, M. Muraguchi, and T. Endoh, "High accurate and low loss current sensing method with novel current path narrowing method for DC-DC converters and its demonstration," in Proc. 2016 IEEE International Telecommunications Energy Conference (INTELEC), pp. 23-27, Oct. 2016.
- [9] R. Channappanavar and S. Mishra, "A novel bidirectional current estimator for digital controlled DC-DC converters," in Proc. IEEE Applied Power Electronics Conference and Exposition (APEC), pp. 3068-3073, Mar. 2018.
- [10] Z.-Y. Hou, H.-C. Tasi, and C.-C. Wang, "High-voltage bidirectional current sensor" in IEEE 12th International Conference on ASIC (ASICON), pp. 1145-1146, Oct. 2017.
- [11] B. Razavi, "Design of Analog CMOS Integrated Circuits," McGraw-Hill College, pp. 308-340, Aug. 2000.
- [12] A123 SYSTEM, "DataSheet: ANR26650m1-B," 2012.
- [13] Y. Jiang, M. Swilam, S. Asar, and A. Fayed, "An accurate sense-FET-based inductor current sensor with wide sensing range for buck converters," in Proc. IEEE International Symposium on Circuits and Systems (ISCAS), pp. 1-4, May 2018.
- [14] LEM, LA 03-PB Datasheet, [Online]. Internet: <https://media.digikey.com/pdf/Data%20Sheets/LEM/newline%20USA%20PDFs/LA%20PDFs/LA%2003%20.%20newline20-PB.pdf>.

TABLE I. Performance Comparison

	[6] TPE	[7] TENCON	[8] INTELEC	[12] ICECS	[13] ISCAS	[14] LEM	This work
Year	2014	2015	2016	2016	2018	N/A	2019
Process	0.5 μm CMOS	0.25 μm BCD	PCB	0.18 μm HVC MOS	0.5 μm CMOS	Hall sensor	T50UHV CMOS
Implementation	Measurement	Measurement	Measurement	Simulation	Simulation	Measurement	Measurement
Bidirectional	No	No	No	No	No	No	Yes
Supply Voltage (V)	5.5	5	12	1.8 & 5	5	± 15	5 ~ 20
Voltage Range (V)	2.7 ~ 4.5	36 ~ 55	1 ~ 12	36	5	± 15	8 ~ 14
Sensing Current Range (A)	0.05 ~ 0.6	0.44 ~ 2.2	0 ~ 20	0.5 ~ 1.5	0 ~ 5	-3 ~ 3	-3 ~ 3
Max. Error (%)	4	2.5	3.3	1.2	3	± 1.5	0.7 ($\leq \pm 3\sigma$)
Core Area (mm ²)	0.05	1.58	N/A	N/A	N/A	N/A	0.78
FOM	4.95	8.17	N/A	N/A	N/A	N/A	76.923

Note: σ : Standard deviation.